RSC Advances

ROYAL SOCIETY OF CHEMISTRY

www.rsc.org/advances

RSC Advances

ARTICLE

A cost-effective polyurethane based activated carbon sponge anode for high-performance microbial fuel cell

Received 00th January 20xx,
Accepted 00th January 20xx

DOI: 10.1039/x0xx00000x

www.rsc.org/

Mengmeng Liu,[a,b] Minghua Zhou,*[a,b] Huijia Yang,[a,b] Yingying Zhao,[a,b] Youshuang Hu[a,b]

A simple and cost-effective three-dimensional (3D) polyurethane based activated carbon sponge (ACS) MFC anode was fabricated by carbon black (CB) deposition and ammonium persulfate (APS)/H_2SO_4 oxidation. This 3D anode (denoted as APS-CB/ACS-SS) possessed remarkable ability with a maximum power density of 926 mW m^{-2}, which was almost 226 folds that of the untreated ACS (4.1 mW m^{-2}) anode, and 2.2 folds compared with conventional carbon cloth anode MFC (414 mW m^{-2}) under the same conditions. Accordingly, the coulombic efficiency (CE) reached 13.4%, increased 538.1% compared with the untreated ACS anode. The results of SEM, FTIR, CV and EIS measurements demonstrated that the performance improvement was related to the changes of surface functional groups introduced by APS/H_2SO_4 oxidation, and the increase of conductivity and catalytic activity by CB coating. This study provided a new approach for cost-effective MFC anode fabrication as well as surface modification to enhance performance.

Introduction

Microbial fuel cell (MFC) is a technology which can potentially address both energy and water quality challenges.[1-3] Various materials are used as MFC anode, and the rapid development of nano-structured electrode opens up new opportunities for high performance MFC,[4-8] attributing to three factors (1) increased surface area, (2) improved electrode biocompatibility, and (3) facilitated electron transfer between electrode and bacteria.[9,10] Although a number of factors affect a MFC's performance, the anode associated with microbial inoculums has the greatest impact on its power density.[11,12] And various anode modification methods have been developed to increase MFC performance, such as acid soaking,[13] high temperature ammonia treatment,[14] heat treatment,[15] electrochemical oxidation,[16,17] and mediator grafting.[18]

Logan and colleagues recently detailed the invention of a graphite fiber brush anode that provides a large specific surface area, depending on the anode size.[19] However, the space between the fibers is not uniformly distributed within the brush and evidence is lacking that full surface of this fiber is accessible for microbial colonization. To further improve MFC performance, 3D open macroporous structure anodes with a large surface area to interface with bacteria, such as textiles,[20] sponges,[21] nickel foam,[22,23] carbon fiber[24], synthetic carbon materials[25] and some carbonized plant material.[26] Compared with conventional flat anodes, they significantly enhance the power output due to open porous structure that has a large bioaccessible surface area, which allows for extensive biofilm formation and efficient transport of nutrients and wastes at the same time. However, the synthetic method for 3D anode was usually complex, and some problems associated include high cost or low biocompatibility or poor conductivity, or disruption of bacteria membrane by sharp nanomaterials.[27] Therefore, low-cost electrodes are still urgently needed to increase MFC performance and reduce capital cost.

Polyurethane based activated carbon sponge (ACS) is an ideal 3D material, which has been used as an excellent support for biofilm growth in water and wastewater treatment.[28] The networked structure can provide a stable support for biofilm attachment while be accessible by bacteria (typical ACS pore is 0.5 - 1 mm and the bacteria size is 0.1 - 3 μm). What's more, the capital cost of the ACS is only \$2.5/m^2 for thickness 3mm, at least one order of magnitude less than the most commercial carbon cloth and 3D carbon mesh electrode.

Account for its low electric conductivity, in the present work, a highly hydrophobic carbon black (CB)[29] was coated to investigate its feasibility as a MFC anode since it was reported that introducing hydrophilic groups on carbon surface could enhance biocompatibility and facilitated the immobilization of bacteria.[30] Further, to improve MFC performance, simple anode oxidation modification method using non-hazardous and economical ammonium persulfate (APS)[31,32] was developed on

[a] Key Laboratory of Pollution Process and Environmental criteria, Ministry of Education, College of Environmental Science and Engineering, Nankai University, Tainjin 30071, China
[b] Key Laboratory of Urban Ecology Environmental Remeidation and Pollution Control, College of Environmental Science and Engineering, Nankai, University, Tianjin 30071, China
†corresponding author. Tel/Fax:+8602266229619.
E-mail Address: zhoumh@nankai.edu.cn(M. Zhou)

this ACS based anode to introduce more hydrophilic groups.[33] Herein, considering that the cost of ACS was almost negligible, a simple and cost-effective 3D ACS based MFC anode was fabricated by CB deposition and chemical oxidation. To the best of our knowledge, this 3D ACS based electrode is for the first time fabricated and applied for MFC. This work demonstrated that this anode performed superior biocompatibility and high electrochemical activity, providing promising alternative anode for MFCs application.

Experimental

Electrode preparation and modification

Deposition CB on ACS. ACS were prepared by activated carbon foaming process on polyurethane sponge (thickness 3mm; pore size 0.5~2mm; Sutong, China) substrates were cut into pieces, and were soaked in hydrochloric acid (1 M) for 24 h to dissolve the adsorbed organics, and then rinsed with ultrapure water. Every 0.5 g ACS was first dispersed in 1.5 mL Nafion solution (5 wt.%, DuPont, USA) and 10 mL deionized water by ultrasonic treatment. Then they were transferred into a beaker filled with 25 mL aqueous CB solution. The autoclave was heated at 120 °C for 5 h and allowed to cool down. This sample was labeled "CB/ACS".

Oxidation of CB/ACS. The CB/ACS was oxidized according to the method in literature.[33] A 1-g quantity of pristine CB/ACS and 20 mL 2.0 mol L^{-1} APS solutions in 1.0 mol L^{-1} H_2SO_4 were added into a 50 mL three-necked round-bottom flask, and maintained at 40 °C for 3 h. The modified ACS was subsequently separated by centrifugation, washed with deionized water until its pH was 6, and then dried in an oven for 1 h at 100 °C. The final sample was labeled "APS-CB/ACS".

Anodes fabrication. To compensate for the conductivity of ACS composite anodes, a stainless-steel (SS) current collector (0.3 mm, Shanhai Hongju Rubber and Plastic Products Co. LTD, China) was attached to the ACS (denoted as ACS-SS, CB/ACS-SS, APS-CB/ACS-SS, respectively). The carbon cloth (CC) (Jilin Shenzhou Carbon Fiber Co. LTD) electrode and SS mesh functioned as a control sample. All the electrodes were fabricated by directly attaching Ti wires onto the carbon-based substrates. The projected areas of all anodes were 7 cm^2.

MFC configuration and operation

A traditional single membrane free single chamber air-cathode MFCs (14 mL volume) was built as previous described.[17]The working electrodes were ACS based anodes (CB/ACS, APS-CB/ACS, ACS-SS, CB/ACS-SS, APS-CB/ACS-SS, respectively). For comparisons, the naked ACS without modification and CC anodes were used as the working electrodes. The space between the anode and cathode is 2.5 cm. The cathode was the Pt/C air cathode (0.3 mg cm^{-2}). MFCs were inoculated with 20% anaerobic sludge (TEDA Sewage Treatment Plant, Tianjin), and a medium containing glucose (1 g L^{-1}) and a 50 mM phosphate buffer solution (PBS: NH_4Cl 0.31 g L^{-1}, KCl 0.13 g L^{-1}, $NaH_2PO_4 \cdot 2H_2O$ 3.32 g L^{-1}, $Na_2HPO_4 \cdot 12H_2O$ 10.36 g L^{-1}) containing vitamins (5 mL L^{-1}) and minerals (12.5 mL L^{-1}). This solution was switched to a feed solution containing glucose (1.0 g L^{-1}) and PBS (50 mM) when the similar output voltage produced over two consecutive cycles. The feed solution was replaced when the voltage dropped below 0.1 V. The external resistance was fixed at 1000 Ω and all tests were operated in duplicate in a fed-batch mode at 30±0.5 °C in a temperature-controlled biochemical incubator. The experiments were run 3 times for each electrode test. To evaluate the stability of the ACS based anode, the MFCs were operated nearly 1 month.

Characterization and analysis

The voltages (V) across the fixed external resistor were measured every minute using a data acquisition system (PISO-813, ICP DAS Co., Ltd.) connected to a personal computer. Polarization curves were obtained by applying a different external resistance (R, from 10000 Ω to 100 Ω) to the circuit and the voltage was recorded for each resistance. Current density (I) was calculated from I=V/R, and normalized to the projected cathode surface area. Power density (P) was calculated using P=IV, and normalized to the projected cathode surface area. Electrochemical measurements were carried out with CHI660D workstation (CH Instruments, Chenhua, Shanghai, China) connected to a personal computer. These tests were conducted in a three-electrode single-chamber reactor containing a working electrode (7 cm^2 projected area), a platinum wire counter electrode, and a SCE reference electrode. Electrochemical activity of the anodic bacteria was measured by cyclic voltammogram (CV) at a scan rate 30 mV/s and electrochemical impedance spectroscopy (EIS; 0.01 Hz to 100 kHz at the open-circuit potential) in the same reactor with the anode as the working electrode, the cathode as the counter electrode, and SCE as the reference electrode. All experiments were performed in 50 mM PBS in the absence of nutrients at room temperature.

The surface morphologies of the anodes before incubation were examined by a field emission scanning electron microscope (FESEM, Hitachi, S-4700). XPS analysis of samples was performed on a PHI5000VersaProbe Quantera X-ray photoelectron spectrometer equipped with a monochromatic PHI670xi Scanning Auger Nanoprobe. Fourier-transform infrared (FTIR) spectra were obtained with Brucker Tensor 27 (German) under ambient conditions. The spectra were obtained in the wavenumber range 4000-600 cm^{-1}. Typically, 64 scans at resolution of 4 cm^{-1} were accumulated for each spectrum. The attenuated total reflection mode with a diamond crystal was used to scan the samples.

The chemical oxygen demand (COD) was measured with the closed reflux spectrophotometric method on a commercial COD detector (HACH, DRB 200, DR/890 Colorimeter, USA). The Coulombic efficiency (CE) was

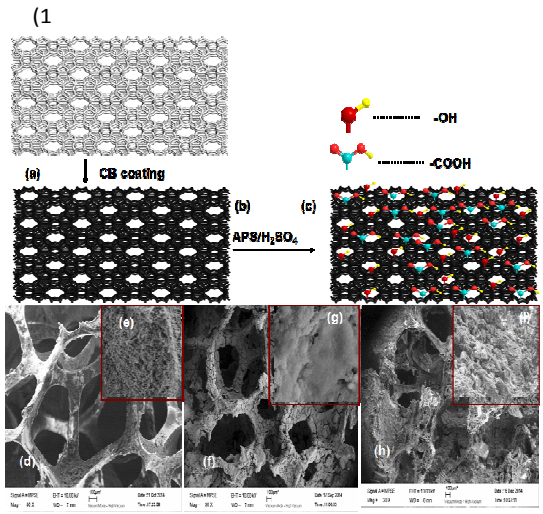

Fig. 1. Conducting APS-CB/ACS anode sponge configuration, fabrication, and characterization. (a) Schematics of a piece of sponge. (b) carbon black are coated onto the ACS. (c) ACS after oxidation by APS /H_2SO_4. (d-e) SEM images showing ACS porous framework before coating. The inset is a high-magnification SEM image showing the ACS's surface after CB coating. (f-g) SEM images showing ACS uniformly coated with CB. The inset is a high-magnification SEM image showing ACS's surface after CB coating. (h-i) SEM images showing CB/ACS after oxidation. Inset is high-magnification SEM image showing surface of CB coating ACS after oxidation.

calculated based on total COD removal (ΔCOD, mg L^{-1}) over the cycle by eq.(1)[3]:

$$CE = \frac{\sum_{i=0}^{t} U_i t_i}{R\Delta COD b F} \times M \qquad (1)$$

Where F is the Faraday constant (96486 C mol^{-1}), U_i is the voltage(V), and t_i is the time(s). R is the external resistance 1000 Ω, b is the number of electrons transferred for oxygen reduction to H_2O (4 mol e^- mol^{-1}), M is the molecular weight of oxygen (32g mol^{-1}).

Results and discussion

Anode surface modification and characterization

Fig. 1 summaries the surface modification involved two key steps. In the first step of coating CB using a simple "hydrothermal deposition" process, the sponges (Fig. 1a) were impregnated into the CB ink, allowing the ink to fill the voids and coat the hydrophilic macroscale pores (Fig. 1b). The second was chemical oxidation of the CB-ACS by APS/H_2SO_4, forming a macroporous hydrophilic layer (Fig. 1c). As illustrated in Fig. 1d, the 3D ACS exhibited a honeycomb structure with a continuous 3D scaffold with a pore size ranging from 500 µm to 2 mm (Fig.1d-1e). The success of CB deposition was confirmed (Fig. 1f-1g), and the thin CB coating did not change the macroporous configuration of the ACS (Fig. 1f). Fig. 1g and Fig. 1h-1i show the SEM images of CB/ACS before and after oxidation. It can be seen that the surface morphology of ACS becomes rougher after treatment, indicating that specific surface area of the CB/ACS would be increased. Some of carbon atoms on the CB/ACS were oxidized and lost through carbon oxide evolution under the APS/H_2SO_4 treatment, resulting in the rougher surface of the electrode.[32] The SEM results indicated that ACS acted as an ideal support for biofilm growth, while the coating of CB would keep high hydrophilic layer for electrode-biofilm interaction.

The XPS of the CB and CB after APS oxidation were shown in Fig. 2. The content of O incresed from 3.53 % to 11.21% after APS oxidation. The C1s peaks of APS-CB (Fig. 2c) displayed a main peak at 284.1 eV, which can be attributed to the sp3-hybridized carbon atoms present in the CB structure[34]. The peak centered at 285.1 eV corresponds to sp2 C=C bonds and is related to defect sites in the CB conjugated rings. The peaks at 286.2, 287.8, and 288.9 eV were assigned to epoxy, carbonyl, and carboxyl groups. Most of the APS-ACS oxygenated groups contained C-O bonds, which can represent, e.g., ether or alcohol moieties. Fig. 2d shows the XPS O1s spectrum, which was further deconvoluted into three components at 531.9, 532.7, and 533.6 eV, thereby confirming the formation of O-H and carboxyl groups on the CB surface[35]. These results are in good agreement with C1peaks of the APS-CB (Fig. 2c).

The FTIR spectra of CB/ACS (Fig. 3a) and its modified composites APS-CB/ACS (Fig. 3b) differ significantly. Bands at approximately 3440 cm^{-1} were observed in the spectra of all samples, which were assigned to O-H stretching vibration.[33,34] An increase in the intensities at 2900 and 2851 cm^{-1} corresponding to aliphatic C-H bonds, was observed. A distinct increase in absorbance between 1580 and 1700 cm^{-1} was observed,

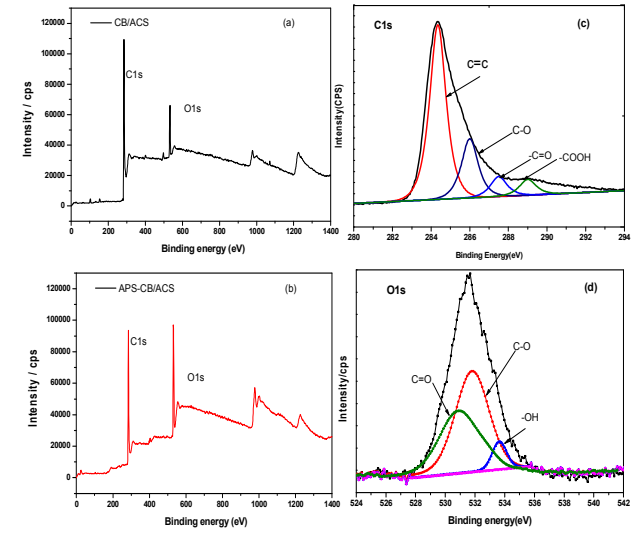

Fig. 2. XPS spectra of CB (a) and APS oxidized CB (b) the XPS deconvoluted XPS C1s peak (c) and O1S peaks (d) of APS-CB.

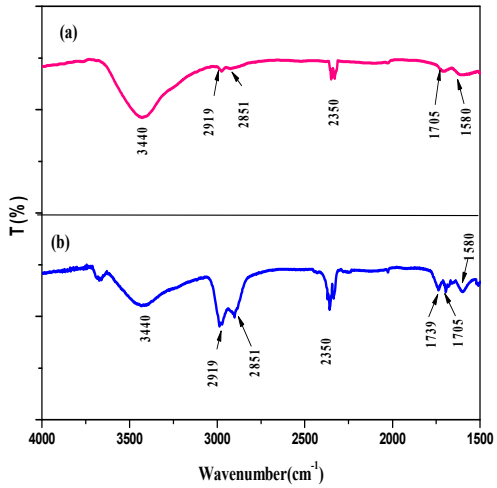

Fig. 3. FTIR of (a) CB/ACS (b) APS-CB/ACS.

which corresponded to the C=O bond, indicating successful oxidation of the electrode.[36] After oxidation, the spectra of the samples included an absorption band at approximately 1700 cm^{-1}, indicating the formation of surface oxygen complexes C=O stretching vibration.[37] The C=O stretching bands appeared at 1705 cm^{-1} in the spectrum of CB/ACS, which are typical of carbonyl groups.[38] In the spectrum of APS-CB/ACS, the same band was shifted to 1739 cm^{-1}. The C=O stretching bands typically appeared at higher wavenumbers when C=O bonds in anhydride, lactone, and carboxylic groups were conjugated with other double bonds and/or aromatic rings. The spectrum of APS-CB/ACS also exhibited increased intensity of the band at approximately 2350 cm^{-1}. This band was typically associated with C=O strength.[38] The oxidation induced a loss of aromaticity in rings of the carbonized product, as deduced from the spectral appearance of two peaks at 2919 and 2851 cm^{-1} that were attributable to σ(C-H) vibrations in C-H groups of the activated product, and the introducing carboxylic acid group into modified anodes would induced more current generation in MFCs.[39,40]

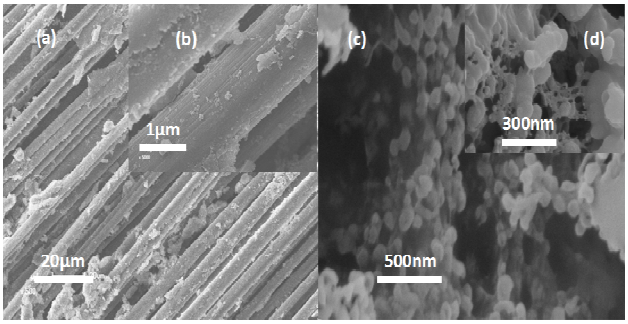

Fig. 4. (a) SEM of carbon cloth; (b) carbon cloth electrode after incubation for 1 month (c) the bacteria was grown inside the 3D electrode for 1 month in MFC. (d) the higher magnification of bacteria.

Growth of bacteria biofilm on anode

Fig. 4 demonstrates the biofilm growth on the CC anode (Fig. 4a, b) and APS-CB/ACS anode (Fig. 4c and Fig. 4d) after 30 days inoculation anodes in a PBS solution (50 mM, pH 7.0). The bacteria can hardly be seen in on the surface CC (Fig. 4a). In Fig. 4c and 4d, a well-developed biofilm can be seen on the interior of the material because lots of bacteria accumulated in the pores of ACS. This occurred in spite of the increased hydrophilicity of the ACS. The result proved that the internal macroporosity of ACS played a crucial role in efficient exploitation of the available surface area. This seems not to be the case for CC anode (Fig. 4a) since the small pore size of CC led to a poor biofilm formation, as seen in Fig. 4b. Although CC was porous, pore diameters was too small (Fig. 4a) and were easily clogged by microbial growth. Further, it could be seen that the bacteria adhesion onto ACS was greater than that for CC, indicating that the ACS based anode was an excellent host for cell growth (Fig. 4c). Thus it could be concluded that the combination of material conductivity and bioaccessible surface area is vital for an efficient anode material. The possible reasons for the improvement were as follows: first, the 3D porous structures were large enough for increases adhesion of bacteria inside. Second, the increase of the acid oxygenous groups on CB could improve the hydrophilicity of the composites.[32] The similar strategy had been adapted when Chen et al. treated CC anode with ammonia to impart hydrogen content on the surface.[14]

Electrochemical behavior of ACS based anode

A more deep insight could be obtained by analyzing EIS and the Nyquist plots (Fig. 5a) to investigate the charge transfer resistance of MFC with the plain CC and ACS based anodes under the same experimental conditions. As shown in Fig. 5a, the charge-transfer resistance of CB/ACS (~440 Ω) was much smaller than the bare ACS (>3000 Ω) indicating that CB coating can efficiently decrease ohmic resistance. The ohmic resistance was further decreased after APS oxidation (227 Ω for APS-CB/ACS). SS was used as current collector since it could increase the electrons transfer but not enable electricity generation and microbial colonization.[20,21] SS is inexpensive, with a conductance several orders of magnitude greater than ACS. The decline in resistance from >3000Ω for ACS to ACS-SS (~130 Ω), can only be attributed to the SS mesh. This confirms the effectiveness of SS as a current collector. The charge-transfer resistance of APS-CB/ACS-SS (~33 Ω) reduced after CB coating, and was further decreased after APS oxidation. The smaller charge-transfer resistance of APS-CB/ACS-SS (~33 Ω) resulted in a faster electron transfer rate. This confirmed that the extracellular electron transfer (EET) efficiency of 3D APS-CB/ACS-SS was higher than that of CC due to the combination of the high conductivity of SS and excellent properties of the hydrophilic CB/ACS.

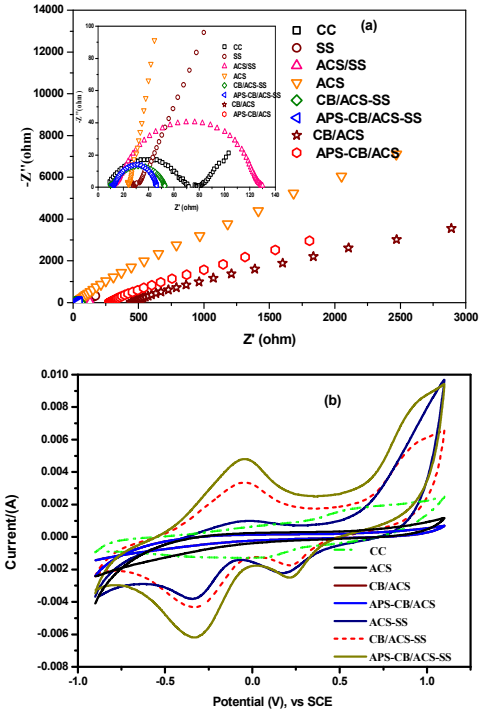

Fig. 5. EIS of MFCs with different anodes (a) and CVs of bacteria on different anodes in a PBS solution (50 mM, pH 7.0) (b).

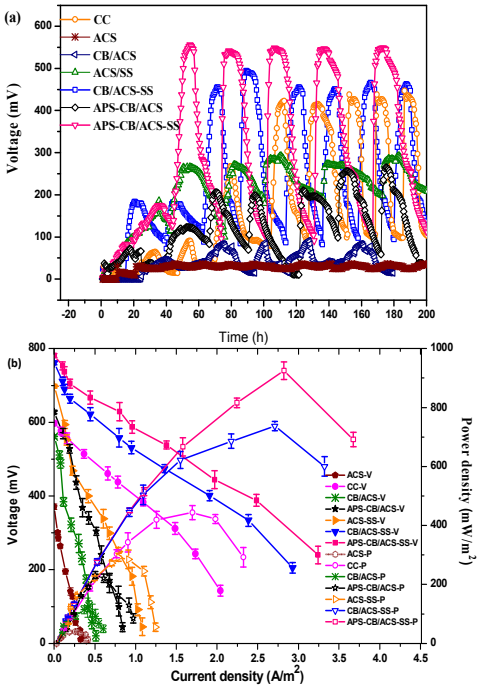

Fig. 6 (a) Voltage output of MFCs with different anodes. (b) Polarization curve and power density curve of MFCs with different anodes.

The differences in CV profiles in Fig. 5b, were due to the differences in the redox peaks which were associated with the amount of redox active components presented within the biofilm. The CV of the ACS-SS, CB/ACS-SS and APS-CB/ACS-SS anodes exhibited several characteristic redox peaks that were missing from that of CC. The SS anode did not show the activity of oxidation of glucose demonstrating the SS did not facilitated formation of the biofilm. However, after the combination of the SS and the ACS, there appeared significant redox current which reflected the electron transfer between the biofilm and anode indicating the biofilm formed on the ACS anode. The peak current increased after the CB coating and further improved after APS oxidation indicating the electrons transfer efficiency enhanced between the anodes and biofilm. The redox peak from -0.4 V to -0.2 V can be produced by the outer membrane C-type *cytochrome* proteins of bacteria that are responsible for the direct electrons transfer between the electrode and the bacteria. The highest peak current, for the APS-CB/ACS-SS anode presented the best bio- and electrocatalysis of the glucose oxidation.

In summary, it can be concluded that the new anode is able to harvest the electrons transfer. These electrochemical analysises demonstrated the advantage of the 3D carbon electrode over the 2D carbon electrodes, suggesting that the coupling effect between 3D ACS and hydrophilic layer was the key to promote electron transfer between bacteria and electrode.

Performance of ACS based anode in a single chamber MFC

The polarization and power density curves obtained from tests in a SCMFC using the 3D APS-CB/ACS-SS anode, which was also compared with that of using CC and the unmodified ACS as anode. As shown in Fig. 6a, the startup time of the APS/H_2SO_4 treatment anode was shorted 23 h, comparing with those untreated anode MFCs. The startup time of APS-CB/ACS-SS MFC was around 56 h while that of CC anode was 112 h.

As shown in Fig. 6b, the maximum power density of ACS was only 41 mW m^{-2}, significantly increased to 207 mW m^{-2} after CB coating and APS oxidation. The power density of CB/ACS increased 77% after APS oxidation. The maximum power density of CB/ACS-SS was 714 mW m^{-2}, significantly increased to 926 mW m^{-2} (APS-CB/ACS-SS) after the APS oxidation, which was about 2.2 times that of CC (414 mW m^{-2}). A maximum current density of 3.27 mA cm^{-2} was reached by APS-CB/ACS-SS, which was 74 times that obtained by ACS anode (0.044 mA cm^{-2}). The maximum voltage of 0.5~0.56V was observed for all the cycles during this month. After 30 days of steady power output, the structure and morphology of the biofilm as shown in Fig 4c, d, the entire surface of the 3D electrode was covered with bacterial cells. Stable operation of the MFCs equipped with ACS based anodes was achieved. These results showed that coupling effect worked when both CB and APS/H_2SO_4 treatment anode were keys to promote the power generation in anode and decrease for the setup time.

The MFC with APS-CB/ACS-SS anode not only showed a very high power production but also demonstrated excellent

COD removal and CE (Fig. 7). The average 20% anaerobic sludge (~1500mg/L) COD decreased 82.2% for the APS-CB/ACS-SS compared to the 62.7% COD removal for CC anode MFC. Higher COD removal at almost the same level feed COD contents due to higher biomass concentration in the column, yielding higher power generation[41]. Microbial activity is strongly affected by the availability of electron donor and requires optimal feeding rate for optimal activity[42]. Therefore, COD removal efficiency of CB/ACS-SS was lower (78.7%) than the APS oxidation anode MFC. This also confirmed the higher biomass adhere to the APS-CB/ACS-SS anode. The anode after oxidation was more favorable for bacteria to grow and multiply. The CE of ACS based anode showed superior to previously studied carbon cloth anode MFCs which were similar in the construction, electrodes area[17]. Such a longer period and higher output voltage led to a high CE for APS-CB/ACS-SS (13.4%) in comparison with the CC (7.8%) and the untreated ACS (2.1%), increased by 71.8% and 538.1%, respectively. The high current production and CE might have come from the relatively high abundances of electrochemical active bacteria and EET efficiency for APS-CB/ACS-SS MFC studies.

The ACS based anode presented superior on COD removal and power output to carbon cloth providing a continuous 3D biocompatibility surface, well stability, excellent mechanical properties. In addition, the preparation of APS-CB/ACS-SS was simple and effective, thus it would provide a cost-effective anode for MFC application.

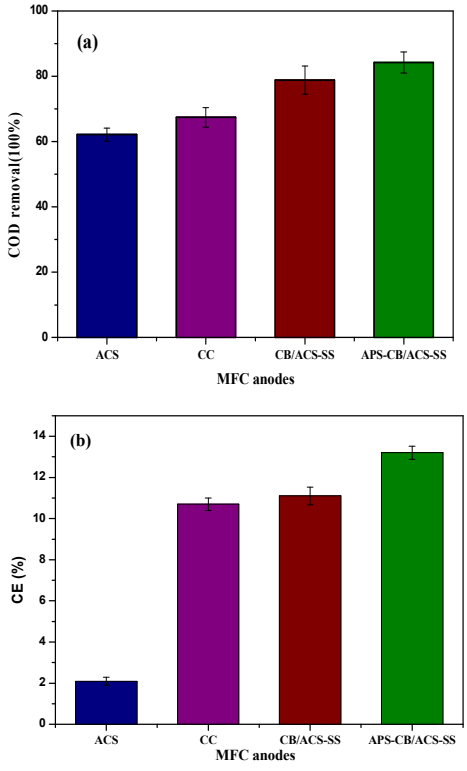

Fig. 7. (a) COD removal efficiency and (b) CE in the MFCs with different anodes.

Conclusions

This study demonstrated that low-cost, energy-efficient CB coated ACS anode could be simply fabricated. The APS/H_2SO_4 oxidization of the composite electrode maximized the oxygen-containing functional groups on creating hydrophilic 3D surfaces, which were favorable for microbial colonization and higher EET efficiency. In comparison with the CC anode, the composites anode delivered 2.2 folds higher output (926 mW m^{-2}) and the setup time shorted 23 h. The CE of the system was 13.4%, increased 538.1% compared to the untreated ACS anode. This work suggested that such a composite anode was promising for improving MFC performance.

Acknowledgements

This work was financially supported by Natural Science Foundation of China (no. 21328602, 51178225 and 21273120), GEFC09-12, and NCET-08-0296.

Notes and references

1 R. A. Bullen, T. C. Arnot, J. B. Lakeman and F. C. Walsh, *Biosens. Bioelectron.,* 2006, **21**, 2015.
2 B. E. Logan, B. Hamelers, R. Rozendal, U. Schrorder, J. Keller, S. Freguia, P. Aelterman, W. Verstraete and K. Rabaey, *Environ. Sci. Technol.*, 2006, **40**, 5181.
3 B. E. Logan and J. M. Regan, *Trends Microbiol.,* 2006, **14**, 512.
4 B. E. Logan, S. Cheng, V. Watson and G. Estadt, *Environ. Sci. Technol.,* 2007, **41**, 3341.
5 I. H. Park, Y.H. Heo, P. Kim, K.H. Nahm, *RSC Adv.,* 2013, **3**, 16665.
6 Z. He, N. Wagner, S. D. Minteer, L. T and Angenent, *Environ. Sci. Technol.,* 2006, **40,** 5212.
7 B. E. Logan, B. Hamelers, R. Rozendal, U. Schroder, J. keller, S. Freguia, P. Aelterman, W. Verstraete and K. Rabaey, *Environ. Sci. Technol.*, 2006, **40**, 5181.
8 M. Zhou, M. Chi, J. Luo, H. He and T. Jin, *J Power Sources,* 2011, **196,** 4427.
9 J. J. Sun, H. Z. Zhao, Q. Z. Yang, J. Song and A. Xue, *Electrochim. Acta,* 2010, **55**, 3041
10 K. Guo, S. Freguia, P.G. Dennis, X. Chen, B. C. Donose, J. Keller, J. J. Gooding and K. Rabaey, *Environ. Sci. Technol.,* 2013, **47**, 7563.
11 B. E. Logan, *Nat. Rev. Microbiol.,* 2009, **7**, 375.
12 W. Zhi, Z. Ge, Z. He and H. Zhang, *Water Res*., 2014, **64,** 32.
13 N. W. Zhu. X. Chen, T. Zhang, P. X. Wu, P. Li and J. H. Wu, *Bioresour. Technol.,* 2011, **102**, 422.
14 S. A. Cheng and B. E. Logan, *Electrochem. Commun.,* 2007, **9**, 492.
15 X. Wang, S. Cheng, Y. J. Feng, M. D. Merrill, T. Saito and B. E. Logan, *Environ. Sci. Technol.,* 2009, **43**, 6870.
16 S. Nambiar, C. A.Togo and J. L. Limson, *Afr. J. Biotechnol.,* 2009, **8**, 6927.
17 M. Zhou, M. Chi, H. Wang and T. Jin, *Biochem. Eng. J.,* 2012, **60**, 151.
18 M. Picot, L. Lapinsonniere, M. Rothballer and F. Barriere, *Biosens. Bioelectron.,* 2011, **28**, 181.
19 B. E. Logan, S. Cheng., V. Watson and G. Estadt., *Environ. Sci. Technol.,* 2007, **41**, 3341.
20 X. Xie, L. Hu, M. Pasta, G. F. Wells, D. Kong, C. S. Criddle and Y. Cui, *Nano Lett.,* 2011, **11**, 291.

21 X. Xie, G. Yu, N. Liu, Z. Bao, C. S. Criddle and Y. Cui, *Energ. Environ. Sci.,* 2012, **5**, 5265.
22 X. Dong, X. Wang, L. Wang,H. Song, H. Zhang, W. Huang and P. Chen, *ACS Appl. Mater. Inter*., 2012, **4**, 3129.
23 H. Wang, Q. Gao and J. Hu, *J. Am. Chem. Soc.,* 2009, **131**, 7016.
24 S. Chen, H. Hou, F. Harnisch, S. A. Patil, A. A. Carmona-Martinez, S. Agarwal, Y. Zhang, S. Sinha-Ray, A. Yarin, A. Greiner and U. Schröder, *Energ. Environ. Sci.,* 2011, **4**, 1417.
25 H. Wang, G. Wang., Y. Ling, F. Qian, Y. Song, X. Lu, S. Chen, Y. Tong and Y. Li, *Nanoscale*, 2013, **5**, 10283.
26 R. Karthikeyan, B. Wang, J. Xuan, J. W. C. Wong, P. K. H. Lee and M. K. H. Leung, *Electrochim. Acta,* 2015, **157**, 314.
27 S. Kang, M. Pinault, L. D. Pfefferle and M. *Elimelech, Langmuir,* 2007, **23**, 8670.
28 P. Chingombe, B. Saha and R. J. Wakeman, *Carbon,* 2005, **43**, 3132.
29 H. Han, J. Lee, D. W. Park and S. E. Shim, *Macromol. Res.,* 2010, **18**, 435.
30 A. Vinu, K. Z. Hossian, P. Srinivasu, M. Miyahara, S. Anandan, N. Gokulakrishnan, T. Mori, K. Ariga and V.V. Balasubramanian, *J. Mater. Chem.,* 2007 **17**, 1819.
31 I. Gniot, P. Kirszensztejn and M. Kozlowski, *Appl. Catal. A: General*, 2009, **362**, 67.
32 B. K. Pradhan and N. K. Sandle, *Carbon,* 1999, **37**, 1323.
33 N. Li, X. Ma, Q. Zha, K. Kim, Y. Chen and C. Song, *Carbon,* 2011, **49**, 5002.
34 S. Biniak, G. Szymanski, J. Siedlewski and A. Swiatkowski, *Carbon*, 1997, **35**, 1799.
35 L. Zhu, Y. Lu, Y. Wang, L, Zhang and W. Wang, *Appl. Surf. Sci*., 2012, **258**, 5387.
36 H. Liu, S. Wen, J. Wang and Y. Zhu, *J. Appl. Polym. Sci.,* 2012, **123**, 3255.
37 J. H. Zhou, Z. J. Sui, J. Zhu, P. Li, D. Chen, Y. C. Dai and W. K. Yuan, *Carbon,* 2007, **45**, 785.
38 M. S. P. Shaffer, X. Fan and A. H. Windle, *Carbon,* 1998, **36**, 1603.
39 S. R. Crittenden,C. J. Sund and J. J Sumner, *Langmuir,* 2006, **22**, 9473.
40 A. J. M. Stams, F.A.M. de Bok, C. M. Plugge, M.H.A. van Eekert, J. Dolfing and G. Schraa, *Environ. Microbiol.,* 2006*,* **8**, 371.
41 L. Yuan, L., W. Zhi, Y. Liu, S. Karyala, P.J. Vikesland, X. Chen and H. Zhang, . *Environ. Sci. Technol.,* 2014, **49**, 824.
42 W. Zhi and G. Ji,. 2014. *Water Res*., 2014, **64**, 32.